A New Simulation Framework to Evaluate Mobility in Dynamic Satellite Networks

Veerendra Kumar Gautam
DEI, University of Padova
Padova, Italy
veerendrakumar.gautam@unipd.it

Marco Giordani
DEI, University of Padova
Padova, Italy
marco.giordani@unipd.it

Dogan Kutay Pekcan
R&D InfoTech Labs
Toyota Motor North America Inc.
dogan.pekcan@toyota.com

Sanjeewa Herath
R&D InfoTech Labs
Toyota Motor North America Inc.
sanjeewa.herath@mail.mcgill.ca

Takayuki Shimizu
R&D InfoTech Labs
Toyota Motor North America Inc.
takayuki.shimizu@toyota.com

Chinmay Mahabal
R&D InfoTech Labs
Toyota Motor North America Inc.
chinmay.mahabal@toyota.com

Chunghan Lee
R&D InfoTech Labs
Toyota Motor North America Inc.
lch@toyota-tokyo.tech

Michele Zorzi
DEI, University of Padova
Padova, Italy
zorzi@dei.unipd.it

***Abstract*—Non-terrestrial networks (NTNs) are a key ingredient of the future 6G ecosystem, enabling global coverage in otherwise unserved areas, as well as continuous and resilient connectivity in case of emergency. Notably, NTNs can be based on Low Earth Orbit (LEO) mega-constellations which, given the close proximity to the Earth, enable a lower latency and higher throughput, compared to constellations at higher altitudes. However, LEO satellites are subject to strong orbital mobility, with velocities on the order of several kilometers per second depending on the altitude. To evaluate the impact of mobility on the protocol stack, accurate and scalable simulation is required. To this aim, in this paper we extend the `ns3-NTN` module, originally developed to simulate satellite networks based on 3GPP Rel. 17+ specifications, to also incorporate satellite mobility using Two-Line Element (TLE) parameters as input for trajectory generation, along with Doppler shift models. The module is validated via extensive ns-3 simulations in terms of throughput, latency, and SNR, considering LEO satellites at 600 km and 1200 km, as well as Geostationary Earth Orbit (GEO) satellites, operating in both S- and Ka-bands. The proposed mobility model is open-source, and enables further research in this domain.**

***Index Terms*—5G NR; Non-Terrestrial Networks (NTN); ns-3; satellite communications; end-to-end simulations; mobility.**

I. Introduction

In the 6G era [1], non-terrestrial networks (NTNs) based on satellites will coexist with terrestrial networks (TNs) to extend coverage in rural and remote regions, and support emergency connectivity in disaster-stricken areas where ground infrastructure is absent or compromised [2]. This paradigm has been formalized by the 3rd Generation Partnership Project (3GPP) since Rel. 17, with a new standard called 5G NR-NTN [3].

Unlike Geostationary Earth Orbit (GEO) satellites, Low Earth Orbit (LEO) satellites operate much closer to the Earth, typically between 300 and 2000 km, which enables lower latency and higher throughput compared to constellations at higher altitudes. However, while GEO satellites remain quasi-stationary relative to the Earth, LEO satellites move rapidly at speeds of several kilometers per second depending on the altitude. This mobility requires frequent handovers, resulting in significant signaling overhead at the Radio Access Network (RAN) and possible service disconnections, and may introduce severe Doppler shifts, especially in the Ka-band (approximately 26.5–40 GHz) [4].

The evaluation of NTNs, including the impact of mobility on the NR-NTN protocol stack, through real-world testbeds is often impractical due to limitations in scalability and flexibility, as well as the high cost of hardware deployment. Consequently, simulation-based approaches in controlled environments have become essential for facilitating research. Among available network simulators, ns-3 enables end-to-end, full-stack performance evaluation with a high degree of customization, and has therefore gained great popularity within the research community. Recently, we released `ns3-NTN` [5], an open-source ns-3 module to simulate satellite networks based on 3GPP Rel. 17 specifications. It implements: (i) the 3GPP NTN channel model, including the effects of path loss, atmospheric absorption, scintillation, and fading at different frequencies (in the S-, L-, and Ka-bands); (ii) multiple antenna models; (iii) an NTN-specific Earth-Centered, Earth-Fixed (ECEF) cartesian coordinate system; and (iv) tailored adjustments to protocol timers based on the characteristics of satellite links. However, the current version of the module does not incorporate realistic satellite mobility.

To date, satellite mobility is predominantly simulated using the NORAD Simplified General Perturbations 4 (SGP4) model [6], which computes the position and velocity of

This work was partially supported by the European Commission through the European Union's Horizon Europe Research and Innovation Programme under the Marie Skłodowska-Curie-SE, GA No. 101129618, UNITE.

satellites at any given time based on orbital parameters (e.g., altitude, inclination, and initial state) derived from Two-Line Element (TLE) data. The outputs of the SGP4 model are expressed in the Earth-Centered Inertial (ECI) frame, a three-dimensional Cartesian coordinate system with its origin at the Earth's center of mass and fixed axes relative to the inertial space. For example, the authors in [7] developed an ns-3 satellite mobility module based on SGP4, even though, unlike our `ns3-NTN` module, it does not model the rest of the NR-NTN protocol stack with the same level of accuracy.

As such, there currently exists no open-source simulation platform able to simulate both accurate full-stack 3GPP NR-NTN protocols and satellite mobility. To fill this gap, in this paper we extend the `ns3-NTN` module to incorporate satellite mobility based on SGP4 TLE parameters. In addition, a time-varying propagation delay model is introduced based on the satellite altitude, and is dynamically updated at regular intervals to capture distance variations between communicating nodes. Moreover, a Doppler shift model is implemented according to the 3GPP TR 38.811 specifications [8], which is a function of the elevation angle and the satellite velocity on the orbit. The accuracy of the module is evaluated via extensive ns-3 simulations in terms of throughput, latency, Packet Delivery Ratio (PDR), and Signal to Noise Ratio (SNR), considering LEO satellites at 600 km and 1200 km, and GEO satellites as a static benchmark, operating in both S- and Ka-bands. The mobility model is open-source, which promotes research in this domain, particularly on the design and evaluation of NTN handover algorithms.

The rest of the paper is organized as follows. In Sec. II we describe the SGP4 mobility and Doppler models. In Sec. III we describe our `ns3-NTN` simulator and new mobility module. In Sec. IV we present simulation results to validate the module. Finally, conclusions are reported in Sec. V.

II. Satellite Mobility and Doppler Models

A. The SGP Mobility Model

The SGP4 model is an analytical orbit propagator used to predict the motion of Earth-orbiting objects over time [6]. It was developed in the 1960s by the U.S. Air Force for space surveillance, and was eventually formalized in the 1970s, building on Brouwer's gravitational theory, incorporating simplified and mathematically-tractable representations of dominant orbital perturbations such as Earth's oblateness and atmospheric drag. Compared to other models, SGP4 offers low computational complexity, making it ideal for large-scale tracking of space objects.

The SGP4 model operates on Two-Line Element (TLE) data, which provide publicly available orbital parameters for Earth-orbiting objects, including satellites. Specifically, a TLE encodes mean orbital elements such as inclination, right ascension of the ascending node (RAAN), i.e., the angular position of the satellite measured along the Earth's equator from a fixed reference direction (typically the vernal equinox), eccentricity, argument of perigee, mean anomaly, mean motion, and a drag-related coefficient. TLE parameters are derived from observational data relative to a certain epoch (as a reference time), combined with simplified dynamical models. Accordingly, the SGP4 model propagates the TLE parameters, i.e., evolves the satellite's orbital state from the TLE reference epoch to a desired time instant, to compute the instantaneous position, velocity, and orbital phase of each satellite in the True Equator Mean Equinox (TEME) reference frame.

B. Doppler Shift

Doppler shift is an important phenomenon in non-geostationary satellite systems, caused by the relative motion, especially the variation in the distance, between the satellite and the ground receiver. This motion introduces a frequency offset that varies over time, which depends on the satellite velocity and position relative to the Earth, and on the frequency f_0.

To model Doppler effects, we adopt the geometric formulation specified in [8], where the satellite and the ground receiver are represented in a Cartesian coordinate system and assumed to lie in the y-z plane. The resulting Doppler shift is calculated and incorporated into the downlink signal model to capture the impact of satellite mobility, particularly in LEO scenarios.

In a circular orbit, the satellite position can be described using the Earth radius R_E, the orbital altitude h, and the elevation angle $\theta(t)$. The corresponding angular velocity of the satellite is given by

$$\omega_{\mathrm{SAT}} = \sqrt{\frac{GM_E}{(R_E + h)^3}}, \tag{1}$$

where G is the gravitational constant, and M_E is the Earth mass. By expressing the relative motion in terms of the elevation angle and simplifying the resulting expression, the Doppler shift can be written in closed form as

$$f_d(t) = \frac{f_0}{c}\, \omega_{\mathrm{SAT}} R_E \cos(\theta(t))\,, \tag{2}$$

where c is the speed of light. This relation shows that the Doppler shift is proportional to the carrier frequency, and varies with the cosine of the elevation angle. As the satellite moves along the orbit, the Doppler shift changes accordingly, becoming more pronounced at lower elevation angles.

III. A New Mobility Module for NTN

A. An Overview of the NTN Simulator

Although significant progress has been made in developing solid theoretical models for NTNs, particularly for the characterization of the satellite channel, experimental and simulation activities remain relatively limited. In particular, existing large-scale NTN simulators are typically closed-source and offer limited flexibility, which makes it difficult for the research community to reproduce results and rigorously evaluate the performance of the proposed protocol designs.

To address these limitations, in 2023 we developed and released `ns3-NTN` [5], an open-source extension of the ns-3 simulator designed for satellite communication networks. In

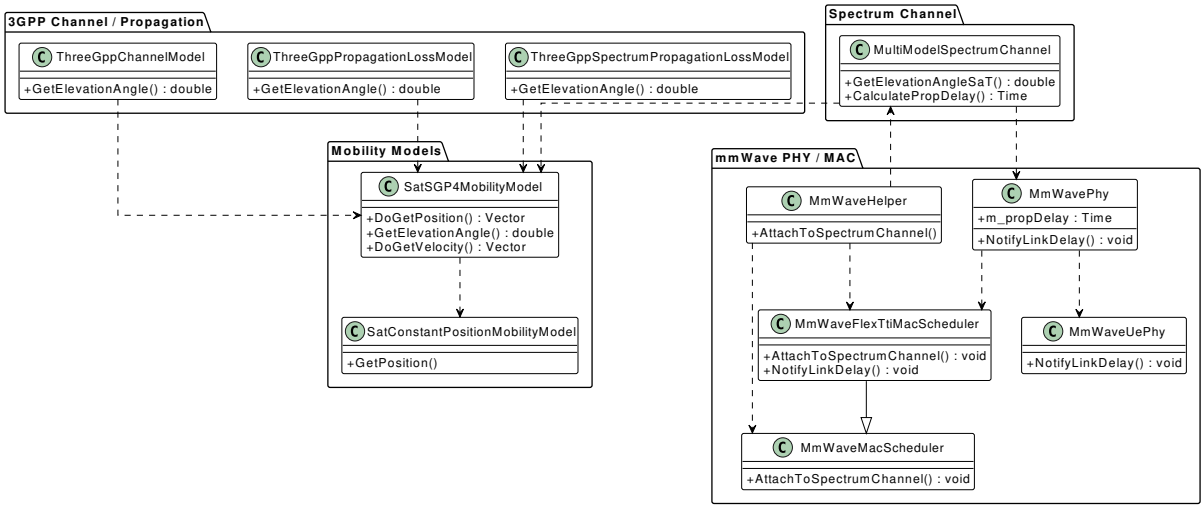


Fig. 1. Simplified UML diagram representing the new classes and methods that have been introduced in the ns3-NTN module to simulate satellite mobility.

contrast to conventional link-level simulators, ns3-NTN enables full-stack, end-to-end simulations, and is aligned with the latest 3GPP 5G NR-NTN specifications. The framework implements the 3GPP TR 38.811 satellite channel model [8], which is based on the baseline TR 38.901 channel model for cellular networks [9]. Specifically, it describes different propagation scenarios for NTN ("Dense Urban," "Urban," "Suburban," and "Rural"), and provides specific path loss, atmospheric absorption, scintillation, and fading models for each of them. Moreover, it incorporates multiple antenna models, including circular aperture, Very Small Aperture Terminal (VSAT), and isotropic antennas. The model uses an ECEF coordinate system to incorporate the effects of Earth's curvature as well as the elevation angle of satellites with respect to the ground. Notably, ns3-NTN is based on the ns3-mmwave module [10] to simulate the rest of the protocol stack according to the 3GPP 5G NR specifications, extending specific protocol timers (especially for HARQ and RRC) to account for the unique features of satellite networks. The module has been evaluated against 3GPP reference results, and was recently integrated into the official ns-3 codebase, starting from release ns-3.42.[1] Still, ns3-NTN introduces some assumptions. In particular, the system operates in Time Division Duplexing (TDD), and is based on Time Division Multiple Access (TDMA). Moreover, the module functions in static conditions, and does not simulate satellite mobility.

B. Description of the Mobility Module

To address the latter limitation, in this work we extended the current implementation of the ns3-NTN module to simulate satellite mobility based on pre-defined satellite orbits. To do so, we developed new classes and methods to model orbital mobility and geometry-dependent propagation delays based on the satellite altitude and elevation angle, as shown in the UML diagram shown in Fig. 1.[2]

a) Satellite mobility: In addition to the baseline SatConstantPositionMobilityModel, in which the positions of a UE and its satellite-gNB are pre-determined a priori and do not change in the simulation, we develop a new SatSGP4MobilityModel where the satellite-gNB moves on pre-defined orbits based on the SGP4 orbital propagation algorithm, as described in Sec. II-A. This class returns the time-varying position and velocity of the satellite using the DoGetPosition() and DoGetVelocity() methods, respectively, which are then used by the channel and propagation models to characterize the satellite link.

b) Channel model: The elevation angle of the satellite influences several channel components, including the path loss, shadowing, and Line-of-Sight (LoS) probability. Because of mobility, the elevation angle changes based on the satellite altitude and the type of orbit. Therefore, the channel modules in the ns3-NTN simulator, namely ThreeGppChannelModel, ThreeGppPropagationLossModel, and ThreeGppSpectrumPropagationLossModel, were extended with a GetElevationAngle() interface. This interface retrieves geometric information from the mobility model, including the satellite elevation angle derived from the current satellite position. The elevation angle is particularly important in NTN channel modeling because several propagation effects, such as atmospheric attenuation and path loss, strongly depend on it. The obtained elevation angle is therefore used in the computation of the corresponding channel parameters.

c) PHY and MAC protocols: While the propagation delay is typically negligible for terrestrial links, in satellite networks it affects several protocol functions, including scheduling, resource allocation, duplexing, and HARQ [4]. To account for this, the MultiModelSpectrumChannel class has been extended with the GetElevationAngleSaT() method to obtain the elevation angle of the satellite at any given time, and the CalculatePropDelay() method to compute the corresponding propagation delay. This class is integrated with the MmWaveHelper, which controls the simulation setup.

[1]https://www.nsnam.org/releases/ns-3-42/.

[2]The mobility module is open-source, and available at https://github.com/VeerendraGautam2025/NTN-Mobility-Model.

TABLE I
SIMULATION PARAMETERS FOR S-BAND (TOP) AND KA-BAND (BOTTOM), BASED ON [8], [11].

S-band						
Parameter	**LEO 600**		**LEO 1200**		**GEO**	
	Satellite	UE	Satellite	UE	Satellite	UE
Carrier frequency	2 GHz		2 GHz		2 GHz	
Bandwidth	30 MHz		30 MHz		30 MHz	
Antenna type	Aperture	Isotropic	Aperture	Isotropic	Aperture	Isotropic
EIRP density	34 dBW/MHz	23 dBm	40 dBW/MHz	23 dBm	59 dBW/MHz	23 dBm
Antenna diameter	2 m	–	2 m	–	22 m	–
Gain	30 dBi	0 dBi	30 dBi	0 dBi	51 dBi	0 dBi
Noise Figure (DL)	–	7 dB	–	7 dB	–	7 dB

Ka-band						
Parameter	**LEO 600**		**LEO 1200**		**GEO**	
	Satellite	UE	Satellite	UE	Satellite	UE
Carrier frequency	20 GHz		20 GHz		20 GHz	
Bandwidth	400 MHz		400 MHz		400 MHz	
Antenna type	Aperture	VSAT	Aperture	VSAT	Aperture	VSAT
EIRP density	4 dBW/MHz	33 dBm	10 dBW/MHz	33 dBm	40 dBW/MHz	33 dBm
Antenna diameter	0.5 m	0.6 m	0.5 m	0.6 m	5 m	0.6 m
Gain	38.5 dBi	39.7 dBi	38.5 dBi	39.7 dBi	58.5 dBi	39.7 dBi
Noise Figure (DL)	–	1.2 dB	–	1.2 dB	–	1.2 dB

TABLE II
SIMULATION PARAMETERS FOR LEO AND GEO SATELLITE SCENARIOS.

Parameter	**LEO 600**	**LEO 1200**	**GEO**
Satellite name	Starlink-550	Starlink-1200	Starlink-GEO
Inclination (deg)	53.0000	53.0000	0.0000
RAAN (deg)	0.0000	0.0000	0.0000
Eccentricity	0.0000001	0.0000001	0.0000001
Argument of perigee (deg)	0.0000	0.0000	0.0000
Mean anomaly (deg)	0.0000	0.0000	0.0000
Mean motion (rev/day)	14.89340181	13.16009679	1.00273907
UE latitude (deg)	-0.0288864		
UE longitude (deg)	-99.9952		
UE altitude (m)	0.0		
Packet size (bytes)	2000		

At the PHY layer, the `MmWavePhy` class now includes an `m_propDelay` attribute to store and update the propagation delay based on the mobility model. This attribute is used to compute the Timing Advance (TA) to compensate for possible time offsets in uplink and downlink, and prevent inter-slot interference. At the MAC layer, the `MmWaveFlexTtiMacScheduler` and `MmWaveMacScheduler` classes are extended with the `AttachToSpectrumChannel()` method, to interface with the `MmWaveHelper` and, consequently, with the `MultiModelSpectrumChannel`, so that scheduling decisions are based on the current link conditions and delay effects.

Finally, the `NotifyLinkDelay()` method is introduced to propagate delay information to the upper layers of the stack.

IV. MODULE EVALUATION VIA SIMULATIONS

A. Simulation Parameters

Simulation parameters are based on the 3GPP technical reports in [8], [11], and are reported in Table I. The scenario consists of a terrestrial UE, wirelessly connected to a satellite at altitude h. We consider LEO satellites at altitudes of 600 km (LEO 600) and 1200 km (LEO 1200), and a GEO satellite at 35 786 km, operating in both the S-band (FR1) and Ka-band (FR2), resulting in six distinct configurations aligned with the 3GPP NR-NTN calibration scenarios. We assume a regenerative payload architecture according to the 3GPP NR-NTN Rel. 19 standard [12], so the satellite operates as a gNB. We consider downlink User Datagram Protocol (UDP) traffic in a rural LoS scenario, with a source rate R.

Satellite parameters are reported in Table II. Specifically, satellites move according to the mobility model described in Sec. II-A, where the elevation angle varies from 90° to 0°. The accuracy of this mobility model will be evaluated in Sec. IV-B via the ns-3 simulator described in Sec. III, as a function of key network metrics such as the end-to-end throughput, latency (measured at the application layer, from packet generation at the gNB to successful reception at the UE), PDR, and SNR. Specifically, the SNR (dB) is calculated as

$$\mathrm{SNR} = \mathrm{EIRP} + G/T - k - \mathrm{PL} - B, \tag{3}$$

where EIRP (dBW) represents the satellite effective isotropic radiated power, which accounts for the antenna transmit power, the cable loss, and the transmit antenna gain, G/T (dB/K) is the receiver antenna gain-to-noise temperature ratio, k (dB/K/Hz) is the Boltzmann constant, PL (dB) accounts for the overall propagation losses (including free-space path loss, atmospheric attenuation, shadowing, and scintillation) [8], and B (dBHz) is the system bandwidth.

B. Simulation Results

Fig. 2 plots the evolution of the downlink end-to-end throughput and the corresponding SNR over time for LEO satellites at 600 km and 1200 km, along with a GEO satellite, in the Ka-band. We observe that the LEO throughput is maximized when the satellite is at zenith (at 90°), and progressively decreases as it moves toward the horizon and the elevation

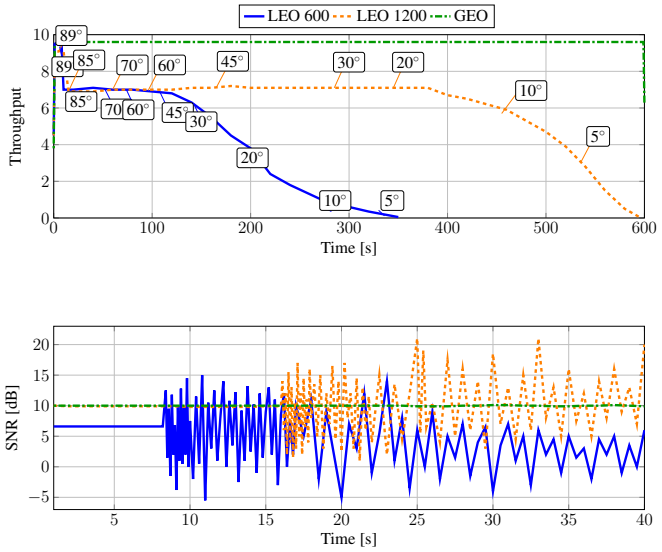


Fig. 2. End-to-end downlink throughput (top), together with the corresponding elevation angles in the box labels, and SNR (bottom) vs. time, considering LEO 600, LEO 1200, and GEO satellites operating in the Ka-band, with a source rate $R = 10$ Mbps.

angle decreases. This trend is consistent with the expected satellite mobility orbital dynamics, and provides a qualitative evaluation of the simulator. Notably, the LEO 1200 satellite remains visible (above the horizon) for approximately 600 s, i.e., about 10 min, whereas the visibility period for a LEO 600 satellite is only around 350 s, i.e., about 6 minutes, given that it moves faster with respect to Earth (7.56 vs. 7.26 km/s). As expected, the performance of the GEO satellite remains nearly constant over time due to its fixed apparent position as seen from the ground. For the LEO satellites, the throughput initially decreases by approximately 20%, as the elevation angle decreases from 90° to around 85°. This trend is also reflected in the SNR in Fig. 2 (bottom), where variability appears after approximately 8 s and 15 s for the LEO 600 and LEO 1200 cases, respectively, as the satellite moves away from zenith. These fluctuations should be attributed to the combined effects of Doppler, fading, and shadowing, that become more severe as the elevation angle decreases. Then, the throughput undergoes a more pronounced degradation once the elevation angle decreases below approximately 45° for LEO 600 and 20° for LEO 1200. In this range, the SNR becomes insufficient to support reliable transmissions, even with the most robust Modulation and Coding Scheme (MCS), leading to frequent link failures. Finally, the link is eventually lost.

Next, Fig. 3 (top) shows the evolution of the end-to-end latency over time. For both the LEO 600 and LEO 1200 configurations, the latency progressively increases as the satellite moves away from zenith. The reason is twofold. First, as the elevation angle decreases, the apparent length of the link (i.e., the slant range) increases, thereby increasing the propagation delay, as depicted in Fig. 3 (bottom). Second, the link quality, and so the channel capacity, decrease, causing packets to accumulate delays in the queue waiting for transmission. Eventually, the latency explodes as the satellite moves out of visibility, i.e., at around 300 s for LEO 600. Notice that

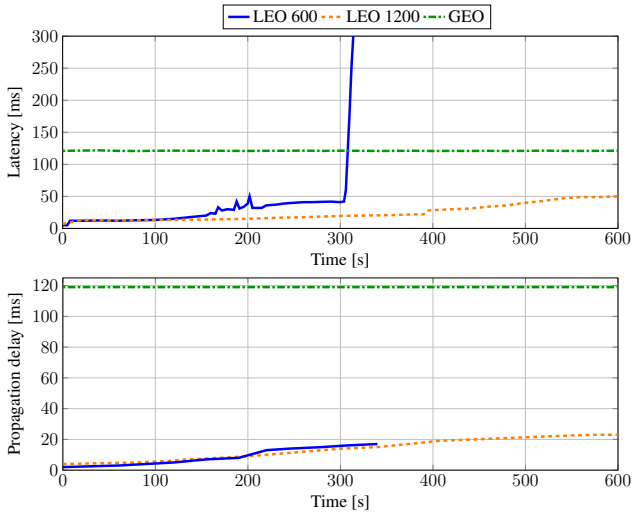


Fig. 3. End-to-end downlink latency (top) and, specifically, the propagation delay (bottom) for LEO 600 km, LEO 1200 km, and GEO satellite links operating in the Ka-band, with a source rate of $R = 10$ Mbps.

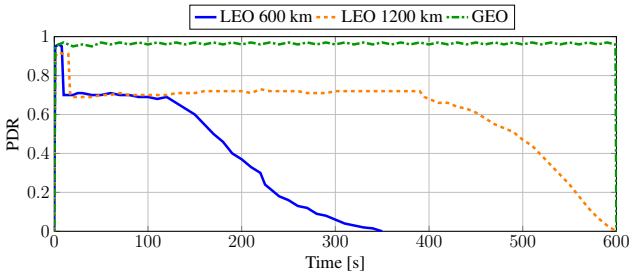


Fig. 4. Packet delivery ratio (PDR) versus time for LEO 600 km, LEO 1200 km, and GEO satellite links operating in the Ka-band, with a source rate of $R = 10$ Mbps.

channel and queuing effects substantially contribute to the end-to-end latency. For example, for LEO 600, the end-to-end latency reaches approximately 50 ms at 300 s, whereas the propagation delay is only about 20 ms. This gap indicates that, at low elevation, latency is dominated by non-propagation components, primarily due to the limited link capacity.

Initially, LEO 1200 has a larger propagation delay than LEO 600 given the greater orbital altitude, as illustrated in Fig. 3 (bottom). However, LEO 600 satellites move faster along the orbit compared to LEO 1200 satellites, which leads to a more rapid increase of the slant range over time. Consequently, after approximately 200 s, the propagation delay of LEO 600 becomes larger than that of LEO 1200, by about 2 ms. Overall, LEO 1200 achieves a lower end-to-end latency than LEO 600, as illustrated in Fig. 3 (top). This difference is also due to the fact that LEO 1200 satellites can operate at higher power (10 vs. 4 dBW/MHz) according to the 3GPP calibration parameters reported in Table I, which improves the link quality.

Similar trends are observed in Fig. 4 for the PDR, which rapidly drops to zero as the elevation angle decreases. In contrast, the performance of the GEO satellite remains stable over time, although with significantly higher latency even at zenith (approximately 125 ms) compared to the LEO configurations due to the longer link.

In Fig. 5 we plot the PDR for a LEO 600 satellite as a function of the application rate R. We see that, after an

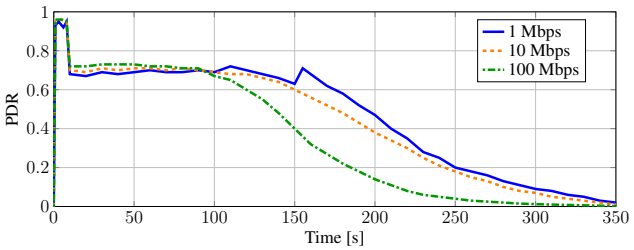


Fig. 5. PDR vs. time as a function of the source rate $R \in \{1, 10, 100\}$ Mbps, considering a LEO 600 satellite operating in the Ka-band.

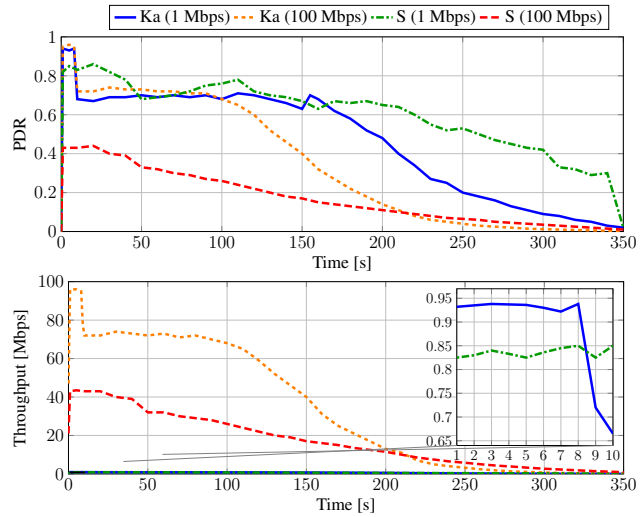


Fig. 6. PDR (top) and end-to-end downlink throughput (bottom) vs. time considering a LEO 600 satellite operating in the Ka- or S-band, sending downlink data with a source rate $R \in \{1, 100\}$ Mbps.

initial degradation due to SNR oscillations, the PDR remains relatively stable, until the network is no longer able to handle the traffic due to congestion. For $R = 1$ Mbps, the PDR starts to decrease at around 150 s, vs. 100 s for $R = 100$ Mbps.

Finally, in Fig. 6 we evaluate throughput and PDR for a LEO 600 satellite operating in either the Ka- or the S-band. The results show that the carrier frequency plays a crucial role on the performance. At high elevation angles, i.e., under favorable link conditions, the end-to-end throughput in the Ka-band is substantially higher than in the S-band, mainly because of the larger available bandwidth (400 vs. 30 MHz). Notably, with a data rate of $R = 100$ Mbps, the PDR in the S-band is only 40%, given that the (limited) available network resources are insufficient to accommodate the requested traffic. However, as the elevation angle decreases, the satellite link in the Ka-band deteriorates more rapidly, and both throughput and PDR drop significantly. This is due to the more severe impact of propagation losses (especially atmospheric absorption and scintillation) in the Ka-band, which reduce the received signal quality and so the channel capacity. Doppler effects are also more pronounced at Ka-band frequencies, which also contributes to rendering the link more unstable. Consequently, below a critical visibility threshold, the S-band provides a more stable throughput, despite the smaller available bandwidth, and represents a more attractive operating option for communication.

V. Conclusions and Future Work

In this work, we implemented a new simulation framework for ns-3 to evaluate satellite mobility at different altitudes. The framework incorporates the SGP4 mobility model based on TLE satellite data, and Doppler-shift effects based on the 3GPP NR-NTN specifications. Using this framework, we conducted a comprehensive simulation campaign in ns-3, evaluating the temporal evolution of end-to-end throughput, latency, PDR, and SNR, for LEO and GEO satellites operating in both S- and Ka-band frequencies. The observed trends are consistent with expected orbital mobility dynamics, which validates the accuracy of our simulator. Specifically, we demonstrated that the Ka-band offers higher throughput under favorable link conditions, while the S-band achieves more stable performance as the link quality deteriorates.

Overall, our results highlight that the network performance strongly depends on the satellite altitude and elevation angle, which affect the entire NR-NTN protocol stack. As part of our future work, we will use the proposed ns-3 framework to design mobility management algorithms for NR-NTN, especially for handover, which would otherwise be difficult to evaluate using standard simulators that do not incorporate accurate mobility models.

References

[1] M. Giordani, M. Polese, M. Mezzavilla, S. Rangan, and M. Zorzi, "Toward 6G Networks: Use Cases and Technologies," *IEEE Communications Magazine*, vol. 58, no. 3, pp. 55–61, March 2020.

[2] M. Giordani and M. Zorzi, "Non-Terrestrial Networks in the 6G Era: Challenges and Opportunities," *IEEE Network*, vol. 35, no. 2, pp. 244–251, Mar./Apr. 2021.

[3] M. Figaro, F. Rossato, M. Giordani, A. Traspadini, T. Shimizu, C. Mahabal, S. Herath, C. Lee, and M. Zorzi, "5G NR Non-Terrestrial Networks: From Early Results to the Road Ahead," *npj Wireless Technology*, vol. 2, no. 31, Jun. 2026.

[4] F. Rossato, M. Figaro, A. Traspadini, T. Shimizu, C. Mahabal, S. Herath, C. Lee, M. Zorzi, and M. Giordani, "5G NR Non-Terrestrial Networks: Open Challenges for Full-Stack Protocol Design," *submitted to the IEEE Communications Magazine*, 2026. [Online]. Available: https://arxiv.org/abs/2601.14883

[5] M. Sandri, M. Pagin, M. Giordani, and M. Zorzi, "Implementation of a channel model for non-terrestrial networks in ns-3," in *ACM Workshop on ns-3*, 2023.

[6] D. Vallado, P. Crawford, R. Hujsak, and T. Kelso, "Revisiting spacetrack report #3," in *AIAA/AAS Astrodynamics Specialist Conference and Exhibit*, 2006, p. 6753.

[7] N. Badini, M. Marchese, and F. Patrone, "NS-3-based 5G Satellite-Terrestrial Integrated Network Simulator," in *IEEE 21st Mediterranean Electrotechnical Conference (MELECON)*, 2022.

[8] 3GPP, "Study on New Radio (NR) to Support Non-Terrestrial Networks (NTN)," TS 38.811, 2021.

[9] 3GPP, "Study on Channel Model for Frequencies from 0.5 to 100 GHz," TS 38.901, 2020.

[10] M. Mezzavilla, M. Zhang, M. Polese, R. Ford, S. Dutta, S. Rangan, and M. Zorzi, "End-to-End Simulation of 5G mmWave Networks," *IEEE Communications Surveys Tutorials*, vol. 20, no. 3, pp. 2237–2263, ThirdQuarter 2018.

[11] 3GPP, "Solutions for NR to Support Non-Terrestrial Networks (NTN)," TS 38.821, 2022.

[12] G. A. Medina-Acosta, T. A. Khan, R. K. Mungara, S. E. Löwenmark, Y. Tan, and Y. Lin, "3GPP Release-19 Physical Layer Enhancements for NR NTN and NB-IoT NTN," *IEEE Communications Standards Magazine*, vol. 10, no. 1, pp. 130–136, Mar. 2026.